Supplement

Supplement of Data

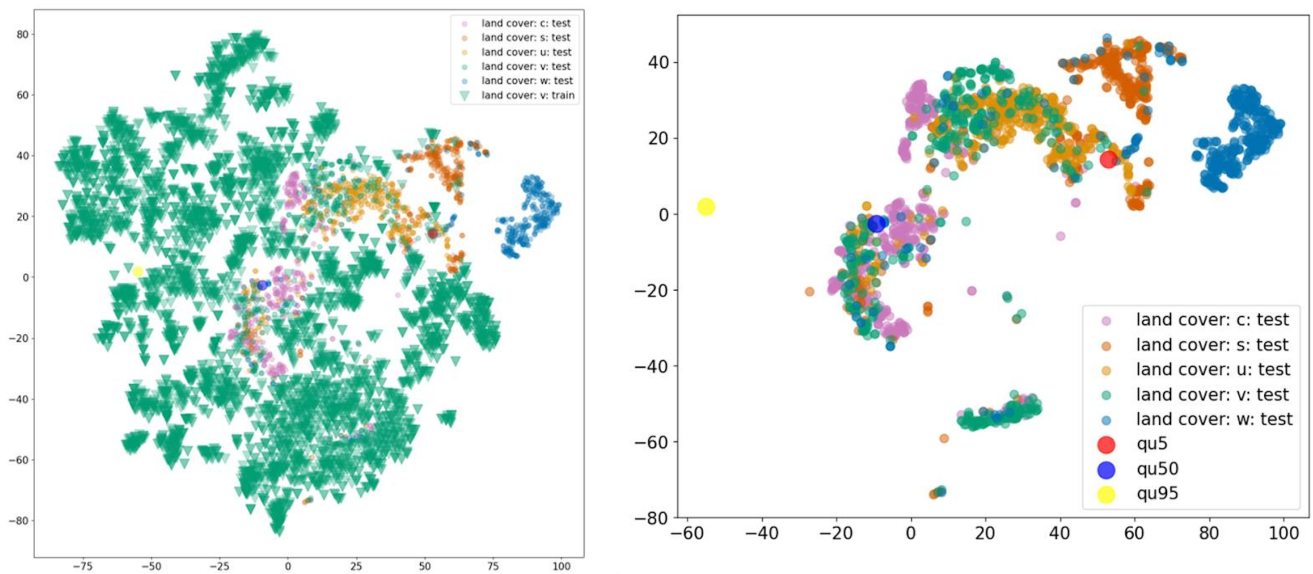

Figure S1: Tsne visualization of the last embedding layer of training vegetation data and out-of-domain (OOD) data. The green triangle points are vegetation points from the training data and the dotted points are samples from an EnMAP scene from different land cover types.

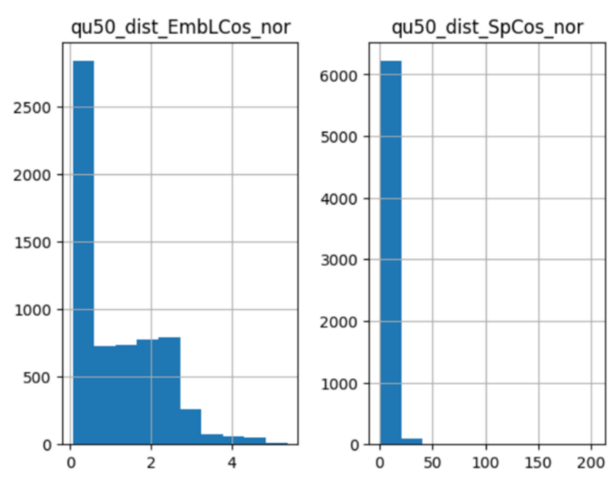

Figure S2: Distribution of the two predictors of uncertainty: normalized median of the cosine distance of 50 neighboring samples in feature space (qu50_distEmbLCos_nor) and the last embedding space (qu50_distSpCos_nor)

Table S1: Number of Training Data Samples by Vegetation Type

LandCover	numSamples
Crops	947
Forest	2639
Grassland	1403
Mix	202
Shrubland	312
Tundra	673
soil	12

Table S2: The distribution of trait observations used for the deep learning model

	LMA	Nitrogen	LAI	Chl	EWT	Car
count	5773	4483	1775	3348	4175	2025
mean	46.38079	0.081173	1.17587	9.422285	6.532881	1.783992
std	62.73074	0.090945	0.976396	8.550426	12.20846	1.673635
min	0.0078	0.000016	0.000424	0.001553	0.008675	0.000512
0.25	8.903973	0.023985	0.448512	3.281224	2.041999	0.611157
0.5	22.74813	0.056672	0.935387	7.347757	4.500577	1.395439
0.75	61.21167	0.106763	1.643611	13.29803	7.879836	2.494338
max	636.6361	1.070588	5.882197	185.2072	487.9816	27.26441

Table S3: Detailed information on the collected Datasets (DSs) for training the deep learning model and their corresponding studies. For some of the data sets, the link between spectra and traits was established based on the dominant species, the sampling plot identifier or the date of measurements according to the data set's available metadata. For the data set with asterisks (DS 17) the weighted species density is used to associate trait values. This table was adopted from Cherif et al. (2023).

Data sets	**Instrument**	**Method**	**Number of bands**	**Land Cover**	**Number of samples**	**Citation**
DS1	ASD FieldSpec® 3 portable spectroradiometer or two SVC HR-1024TM	Proximal canopy measurements	2151	Grassland	73	Van Cleemput E., Helsen K., Feilhauer H., Honnay H. and Somers B.. 2020. Canopy spectra of individual herbaceous species measured on black table. Data set. Available online [http://ecosis.org] from the Ecological Spectral Information System (EcoSIS). doi:10.21232/ss03-g783
DS2,3	ASD Fieldspec3	Proximal canopy measurements	2101	Grassland	658	Kattenborn T. Schiefer F. Schmidtlein S.. 2017. Canopy reflectance plant functional gradient IFGG/KIT. Data set. Available online [http://ecosis.org] from the Ecological Spectral Information System (EcoSIS). doi:10.21232/krt4-6x67
DS4	ASD Fieldspec3	Proximal canopy measurements	2151	Grassland	549	Van Cleemput E., Roberts D. A., Honnay O. and Somers B.. 2019. Individual forb and grass species spectra measured on field patches and on a black table. Data set. Available online [http://ecosis.org] from the Ecological Spectral Information System (EcoSIS). doi:10.21232/ntk7-zn04

DS5	Spectra Vista Corporation (SVC) HR-1024i spectroradiometer	Proximal canopy measurements	2151	Tundra	511	Shawn P. Serbin Daryl Yang Ran Meng Andrew McMahon Wouter Hantson Daniel Hayes Kim Ely. 2017. NGEE Arctic 2017 Canopy Spectral Reflectance Seward Peninsula Alaska. Data set. Available online [http://ecosis.org] from the Ecological Spectral Information System (EcoSIS)
DS6	Spectra Vista Corporation (SVC) HR-1024i spectroradiometer	Proximal canopy measurements	2151	Tundra	129	Shawn P. Serbin Daryl Yang Wouter Hantson Kim S. Ely. 2019. NGEE Arctic 2019 Canopy Spectral Reflectance Seward Peninsula Alaska. Data set. Available online [http://ecosis.org] from the Ecological Spectral Information System (EcoSIS)
DS7 & 30-42	AVIRIS next-gen	Airborne	426	Mix	1126	Zhihui Wang. Canopy Spectra to Map Foliar Functional Traits over NEON domains in eastern United States. Data set. Available online [http://ecosis.org] from the Ecological Spectral 9Information System (EcoSIS). doi:10.21232/e2jt-520
DS8	Spectra Vista Corporation (SVC) HR-1024i spectroradiometer	Proximal canopy measurements	2151	Tundra	43	Shawn P. Serbin Alistair Rogers Kim Ely. 2016. NGEE Arctic 2016 Averaged Canopy Spectral Reflectance Seward Peninsula Alaska. Data set. Available online [http://ecosis.org] from the Ecological Spectral Information System (EcoSIS)
DS9	Spectra Vista Corporation (SVC) HR-2014i and Spectral Evolution (SE) PSR+ instrument	Proximal canopy measurements	2151	Tundra	178	Shawn Serbin Wil Lieberman-Cribbin Kim Ely Alistair Rogers. NGEE Arctic BNL Canopy Spectral Reflectance Utqiagvik (Barrow) Alaska 2014 to 2016. Data set. Available online [http://ecosis.org] from the Ecological Spectral Information System (EcoSIS)

DS10	Spectra Vista Corporation (SVC) HR-1024i spectroradiometer	Proximal canopy measurements	2151	Shrubland	22	Shawn P. Serbin Daryl Yang Ran Meng Andrew McMahon Wouter Hantson Daniel Hayes Kim Ely. 2018. NGEE Arctic 2018 Canopy Spectral Reflectance Kougarok Watershed Seward Peninsula Alaska. Data set. Available online [http://ecosis.org] from the Ecological Spectral Information System (EcoSIS)
DS11	Spectral evolution (PSR+)	Proximal canopy measurements	2151	Crops	174	Angela C Burnett Shawn P Serbin Alistair Rogers. 2020. Leaf and canopy spectroscopy and biochemical data of field-grown Cucurbita pepo under two stresses. Data set. Available online [http://ecosis.org] from the Ecological Spectral Information System (EcoSIS). 10.21232/RLmYbmE3
DS12&15	AVIRIS-Classic	Airborne	223	Forest (broad- and needle-leaf)	304	Aditya Singh. 2015. Mapping Canopy Foliar Chemical and Morphological Traits Using Imaging Spectroscopy. Data set. Available online [http://ecosis.org] from the Ecological Spectral Information System (EcoSIS)
DS13	ASD FieldSpec Pro FR	Proximal canopy measurements	2011	Crops	330	Agustin Pimstein David J Bonfil Arnon Karnieli. 2004 and 2005. Wheat Canopy Spectra Collected Throughout Growing Season. Data set. Available online [http://ecosis.org] from the Ecological Spectral Information System (EcoSIS)
DS14	NEON AOP	Airborne	351	Forests (temperate broadleaf)	59	Chlus et al.. 2020. 3D LMA Canopy Level Spectra. Data set. Available online [http://ecosis.org] from the Ecological Spectral Information System (EcoSIS)

DS16	FieldSpec3	Proximal canopy measurements	1950	Grassland	96	Cerasoli, S., Campagnolo, M., Faria, J., Nogueira, C., and Caldeira, M. D. C.: On estimating the gross primary productivity of Mediterranean grasslands under different fertilization regimes using vegetation indices and hyperspectral reflectance, Biogeosciences, 15, 5455–5471, https://doi.org/10.5194/bg-15-5455-2018
DS17 *	AISA Dual system (Specim, Ltd. Finland)	Airborne	75	Grasslands	70	Pottier, Julien et al. (2014), Data from: Modelling plant species distribution in alpine grasslands using airborne imaging spectroscopy, Dryad, Dataset, https://doi.org/10.5061/dryad.n13hn
DS18	HySpex	Airborne	332	Crops	32	Hank, Tobias Benedikt; Locherer, Matthias; Richter, Katja; Mauser, Wolfram (2016): Neusling (Landau a.d. Isar) 2012 - A Multitemporal and Multisensoral Agricultural EnMAP Preparatory Flight Campaign (Datasets). V. 1.2. GFZ Data Services. https://doi.org/10.5880/enmap.2016.007
DS19	HySpex	Airborne	332	Crops	91	Hank, Tobias Benedikt; Locherer, Matthias; Richter, Katja; Mauser, Wolfram (2016): Neusling (Landau a.d. Isar) 2012 - A Multitemporal and Multisensoral Agricultural EnMAP Preparatory Flight Campaign (Datasets). V. 1.2. GFZ Data Services. https://doi.org/10.5880/enmap.2016.007
DS20	HyMap	Airborne	125	Crops	147	Hank, Tobias Benedikt; Richter, Katja; Mauser, Wolfram (2015): Neusling (Landau a.d. Isar) 2009 - An Agricultural EnMAP Preparatory Flight Campaign Using the HyMap Instrument (Datasets). GFZ Data

						Services. https://doi.org/10.5880/enmap.2015.002
DS21	HyMap	Airborne	125	Crops	127	Hank, Tobias Benedikt; Richter, Katja; Mauser, Wolfram (2015): Neusling (Landau a.d. Isar) 2009 - An Agricultural EnMAP Preparatory Flight Campaign Using the HyMap Instrument (Datasets). GFZ Data Services. https://doi.org/10.5880/enmap.2015.002
DS22	Apex	Airborne	288	Crops	106	Hank, Tobias Benedikt; Richter, Katja; Locherer, Matthias; Frank, Toni; Mauser, Wolfram (2015): Neusling (Landau a.d. Isar) 2011 - An Agricultural EnMAP Preparatory Flight Campaign Using the APEX Instrument (Datasets). GFZ Data Services. https://doi.org/10.5880/enmap.2015.003
DS23	ASD FieldSpec 3 JR	Proximal canopy measurements	2151	Crops	18	Wocher, M.; Berger, K.; Danner, M.; Mauser, W.; Hank, T. Physically-Based Retrieval of Canopy Equivalent Water Thickness Using Hyperspectral Data. Remote Sens. 2018, 10, 1924. https://doi.org/10.3390/rs10121924
DS25	APEX	Airborne	248	Forest	50	Ewald, M., Skowronek, S., Aerts, R. et al. Analyzing remotely sensed structural and chemical canopy traits of a forest invaded by Prunus serotina over multiple spatial scales. Biol Invasions 20, 2257–2271 (2018). https://doi.org/10.1007/s10530-018-1700-9

DS26	APEX	Airborne	233	Grassland	90	Ewald, M., Skowronek, S., Aerts, R., Lenoir, J., Feilhauer, H., van de Kerchove, R., Honnay, O., Somers, B., Garzón-López, C.X., Rocchini, D., others, 2020. Assessing the impact of an invasive bryophyte on plant species richness using high resolution imaging spectroscopy. Ecol Indic 110, 105882. https://doi.org/10.1016/j.ecolind.2019.105882
DS27	NEO spectrometer	Airborne	187	Forest	80	Adam Chlus and Philip A. Townsend. Seasonal canopy spectra and traits, Blackhawk Island, WI. Data set. Available on-line [http://ecosis.org] from the Ecological Spectral Information System (EcoSIS)
DS28	HrHSI	Airborne	2150	Grassland	60	Dao, P.D., Axiotis, A. and He, Y., 2021. Mapping native and invasive grassland species and characterizing topography-driven species dynamics using high spatial resolution hyperspectral imagery. International Journal of Applied Earth Observation and Geoinformation, 104, p.102542.
DS29	ASD FieldSpec 3	Proximal canopy measurements	2150	Mix	173	Jessica McCarty Amanda Grimm. 2017. Hawaii Volcanoes National Park February 2017 Spectra. Data set. Available on-line [http://ecosis.org] from the Ecological Spectral Information System (EcoSIS)
DS43	ASD	Proximal canopy measurements	2150	Forest, Crops	24	Dar Roberts. Canopy-level reflectance spectra and leaf area for poplars in Washington. Data set. Available on-line [http://ecosis.org] from the Ecological Spectral Information System (EcoSIS)

DS44	AisaFENIX	Airborne	627	Crops	45	Brown, L. A., Morris, H., MacLachlan, A., D'Adamo, F., Adams, J., Lopez-Baeza, E., Albero, E., Martínez, B., Sánchez-Ruiz, S., Campos-Taberner, M., and others: Hyperspectral leaf area index and chlorophyll retrieval over forest and row-structured vineyard canopies, Remote Sens. (Basel), 16, 2066, 2024.
DS45	AisaFENIX	Airborne	622	Forest	47	Brown, L. A., Morris, H., MacLachlan, A., D'Adamo, F., Adams, J., Lopez-Baeza, E., Albero, E., Martínez, B., Sánchez-Ruiz, S., Campos-Taberner, M., and others: Hyperspectral leaf area index and chlorophyll retrieval over forest and row-structured vineyard canopies, Remote Sens. (Basel), 16, 2066, 2024.
DS46	AVIRIS-NG	Airborne	425	Forest	28	
DS47	Casi+Sasi	Airborne	220	Forest	166	Gravel, A., Laliberté, E., Kalacska, M. (2024). Foliar Functional Trait Mapping of a mixed temperate forest using imaging spectroscopy. Federated Research Data Repository. https://doi.org/10.20383/103.0922
DS48	AVIRIS-NG	Airborne	360	Forest	96	Ting Zheng, Zhiwei Ye , Aditya Singh, Ankur R. Desai, N.S.R. Krishnayya, Maulik G. Dave and Philip A. Townsend. 2023. Plot level traits and their corresponding image spectra from the Western Ghats of India. Data set. Available on-line [http://ecosis.org] from the Ecological Spectral Information System (EcoSIS). 10.21232/5nt5bd9p

DS49	MSV 500 + Middleton, Spectral Vision	Proximal canopy measurements	768	Crops	94	Wang, D. R., Wolfrum, E. J., Virk, P., Ismail, A., Greenberg, A. J., & McCouch, S. R. (2016). Robust phenotyping strategies for evaluation of stem non-structural carbohydrates (NSC) in rice. Journal of Experimental Botany, 67(21), 6125–6138. https://doi.org/10.1093/jxb/erw375
DS50	AVIRIS-NG (SHIFT)	Airborne	427	Forest	1825	Brodrick, P.G., R. Pavlick, M. Bernas, J.W. Chapman, R. Eckert, M. Helmlinger, M. Hess-Flores, L.M. Rios, F.D. Schneider, M.M. Smyth, M. Eastwood, R.O. Green, D.R. Thompson, K.D. Chadwick, and D.S. Schimel. 2023. SHIFT: AVIRIS-NG L2A Unrectified Surface Reflectance Version 1. ORNL DAAC, Oak Ridge, Tennessee, USA. https://doi.org/10.3334/ORNLDAAC/2376 Chadwick, K.D., N. Queally, T. Zheng, J. Cryer, C. Vanden Heuvel, C. Villanueva-Weeks, C. Ade, L. Anderegg, Y. Angel, B. Baker, I. Boving, R.K. Braghiere, P. Brodrick, P. Campbell, K.C. Cushman, F.W. Davis, P.D. Dao, A. Dibartolo, R. Eckert, K. Grant, B. Heberlein, M. Johnson, J. Joutras, C. Kibler, M. Klope, K. Kovach, A. Kreisberg, P. Lovegreen, A.J. Maguire, C. Mcmahon, K. Miner, C. Nickles, F. Ochoa, J.P. OcÃƒÆ’Ã‚Â³n, A. Ongjoco, E. Ordway, M. Park, R. Pavlick, A.M. Raiho, D.A. Roberts, D.S. Schimel, F.D. Schneider, K. Thompson, P. Townsend, E. Vermeer, N. Vinod, and K. Zumdahl. 2023. SHIFT: Photosynthetic and Leaf Traits, Santa Barbara County, 2022.

						ORNL DAAC, Oak Ridge, Tennessee, USA. https://doi.org/10.3334/ORNLDAAC/2233

References

Brodrick, P. G., Pavlick, R., Bernas, M., Chapman, J. W., Eckert, R., Helmlinger, M., Hess-Flores, M., Rios, L. M., Schneider, F. D., Smyth, M. M., Eastwood, M., Green, R. O., Thompson, D. R., Chadwick, K. D., and Schimel, D. S.: SHIFT: AVIRIS-NG L2A Unrectified Surface Reflectance Version 1, ORNL DAAC, Oak Ridge, Tennessee, USA, 2023.

Brown, L. A., Camacho, F., García-Santos, V., Origo, N., Fuster, B., Morris, H., Pastor-Guzman, J., Sánchez-Zapero, J., Morrone, R., Ryder, J., and others: Fiducial Reference Measurements for Vegetation Bio-Geophysical Variables: An End-to-End Uncertainty Evaluation Framework, Remote Sens. (Basel), 13, 3194, 2021.

Brown, L. A., Dash, J., Lidón, A. L., Lopez-Baeza, E., and Dransfeld, S.: Synergetic exploitation of the Sentinel-2 missions for validating the Sentinel-3 Ocean and Land Color Instrument terrestrial chlorophyll index over a vineyard dominated Mediterranean environment, IEEE J. Sel. Top. Appl. Earth Obs. Remote Sens., 12, 2244–2251, 2019.

Burnett, A. C., Serbin, S. P., and Rogers, A.: Source-sink imbalance detected with leaf- and canopy-level spectroscopy in a field-grown crop, Plant Cell Environ., 44, 2466–2479, 2021.

Cerasoli, S., Campagnolo, M., Faria, J., Nogueira, C., and Caldeira, M. C.: On estimating the gross primary productivity of Mediterranean grasslands under different fertilization regimes using vegetation indices and hyperspectral reflectance, Biogeosciences, 15, 5455–5471, 2018.

Chadwick, K. D., Queally, N., Zheng, T., Cryer, J., Vanden Heuvel, C., Villanueva-Weeks, C., Ade, C., Anderegg, L., Angel, Y., Baker, B., and others: SHIFT: Photosynthetic and Leaf Traits, Santa Barbara County, 2022, ORNL DAAC, Oak Ridge, Tennessee, USA, 2023.

Chlus, A., Kruger, E. L., and Townsend, P. A.: Mapping three-dimensional variation in leaf mass per area with imaging spectroscopy and LiDAR in a temperate broadleaf forest, Remote Sens. Environ., 250, 112043, 2020.

Dao, P. D., Axiotis, A., and He, Y.: Mapping native and invasive grassland species and characterizing topography-driven species dynamics using high spatial resolution hyperspectral imagery, Int. J. Appl. Earth Obs. Geoinf., 104, 102542, 2021.

Ewald, M., Skowronek, S., Aerts, R., Dolos, K., Lenoir, J., and others: Analyzing remotely sensed structural and chemical canopy traits of a forest invaded by Prunus serotina over multiple spatial scales, Biol. Invasions, 20, 2257–2271, 2018.

Ewald, M., Skowronek, S., Aerts, R., Lenoir, J., Feilhauer, H., and others: Assessing the impact of an invasive bryophyte on plant species richness using high-resolution imaging spectroscopy, Ecol. Indic., 110, 105882, 2020.

Gravel, A., Laliberté, E., and Kalacska, M.: Foliar functional trait mapping of a mixed temperate forest using imaging spectroscopy, Federated Research Data Repository, 2024.

Hank, T., Locherer, M., Richter, K., Mauser, W., Consortium, E., and others: Neusling (Landau ad Isar) 2012—a multitemporal and multisensoral agricultural EnMAP Preparatory Flight Campaign, 2016.

Hank, T., Richter, K., Mauser, W., Consortium, E., and others: Neusling (Landau ad Isar) 2009—an agricultural EnMAP Preparatory Flight Campaign using the HyMap instrument, 2015.

Herrmann, I., Pimstein, A., Karnieli, A., Cohen, Y., Alchanatis, V., and Bonfil, D. J.: LAI assessment of wheat and potato crops by VENμS and Sentinel-2 bands, Remote Sens. Environ., 115, 2141–2151, 2011.

Kattenborn, T., Fassnacht, F. E., and Schmidtlein, S.: Differentiating plant functional types using reflectance: Which traits make the difference?, Remote Sens. Ecol. Conserv., 5, 5–19, 2019.

Lichtenthaler, H. K.: Chlorophylls and carotenoids: pigments of photosynthetic biomembranes, in: Methods in Enzymology, Vol. 148, 350–382, Elsevier, 1987.

Pottier, J., Malenovský, Z., Psomas, A., Homolová, L., Schaepman, M. E., and others: Modelling plant species distribution in alpine grasslands using airborne imaging spectroscopy, Biol. Lett., 10, 20140347, 2014.

Rogers, A., Serbin, S., and Ely, K.: Leaf mass area, leaf carbon and nitrogen content, Kougarok Road and Teller Road, Seward Peninsula, Alaska, 2016, 2021.

Singh, A., Serbin, S. P., McNeil, B. E., Kingdon, C. C., and Townsend, P. A.: Imaging spectroscopy algorithms for mapping canopy foliar chemical and morphological traits and their uncertainties, Ecol. Appl., 25, 2180–2197, 2015.

Zheng, T., Ye, Z., Singh, A., Desai, A. R., Krishnayya, N. S. R., Dave, M. G., and Townsend, P. A.: Plot-level traits and their corresponding image spectra from the Western Ghats of India, Ecological Spectral Information System (EcoSIS), 2023.

van Cleemput, E., Roberts, D. A., Honnay, O., and Somers, B.: A novel procedure for measuring functional traits of herbaceous species through field spectroscopy, Methods Ecol. Evol., 10, 1332–1338, 2019.

Wang, D. R., Wolfrum, E. J., Virk, P., Ismail, A., Greenberg, A. J., and McCouch, S. R.: Robust phenotyping strategies for evaluation of stem non-structural carbohydrates (NSC) in rice, J. Exp. Bot., 67, 6125–6138, 2016.

Wang, Z., Chlus, A., Geygan, R., Ye, Z., Zheng, T., Singh, A., and others: Foliar functional traits from imaging spectroscopy across biomes in eastern North America, New Phytol., 228, 494–511, 2020.

Wocher, M., Berger, K., Danner, M., Mauser, W., and Hank, T.: Physically-based retrieval of canopy equivalent water thickness using hyperspectral data, Remote Sens. (Basel), 10, 1924, 2018.

Supplement of the distance-based uncertainty modelling

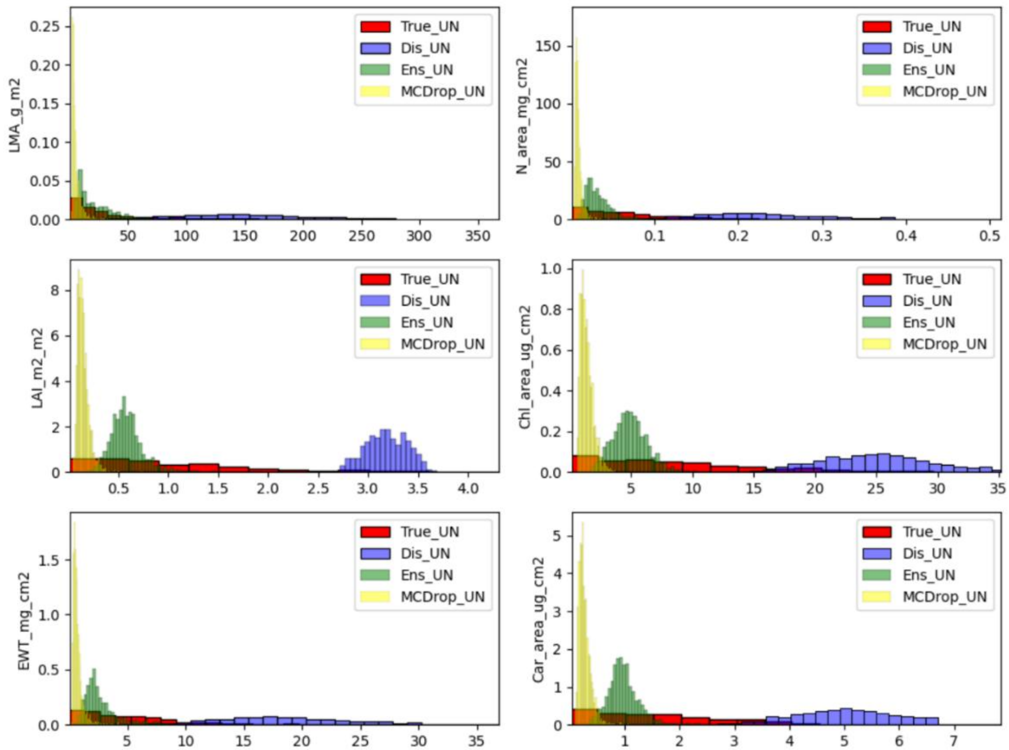

Figure S3: Density distribution of the uncertainty prediction values of three uncertainty models with OOD vegetation data: the distance-based method (Dis_UN), ensemble deep learning (Ens_UN) and monte carlo drop-out method (MCDrop_UN)

Table S4: The ratio coefficient of all traits as calculated with Eq. (2): predicted ranges over the observed residuals of three uncertainty models with OOD vegetation data: the distance-based method (Dis_UN), ensemble deep learning (Ens_UN) and monte carlo drop-out method (MCDrop_UN)

Traits	Dist_UN	Ens_Un	Mcdrop_UN
LMA	107.446	28.817	6.108
N	86.692	26.535	5.09
LAI	22.554	27.591	6.059
Chl	65.518	22.026	6.464
EWT	77.913	30.646	6.618
Car	65.443	24.766	8.511
AVG	**70.928**	**26.73**	**6.475**

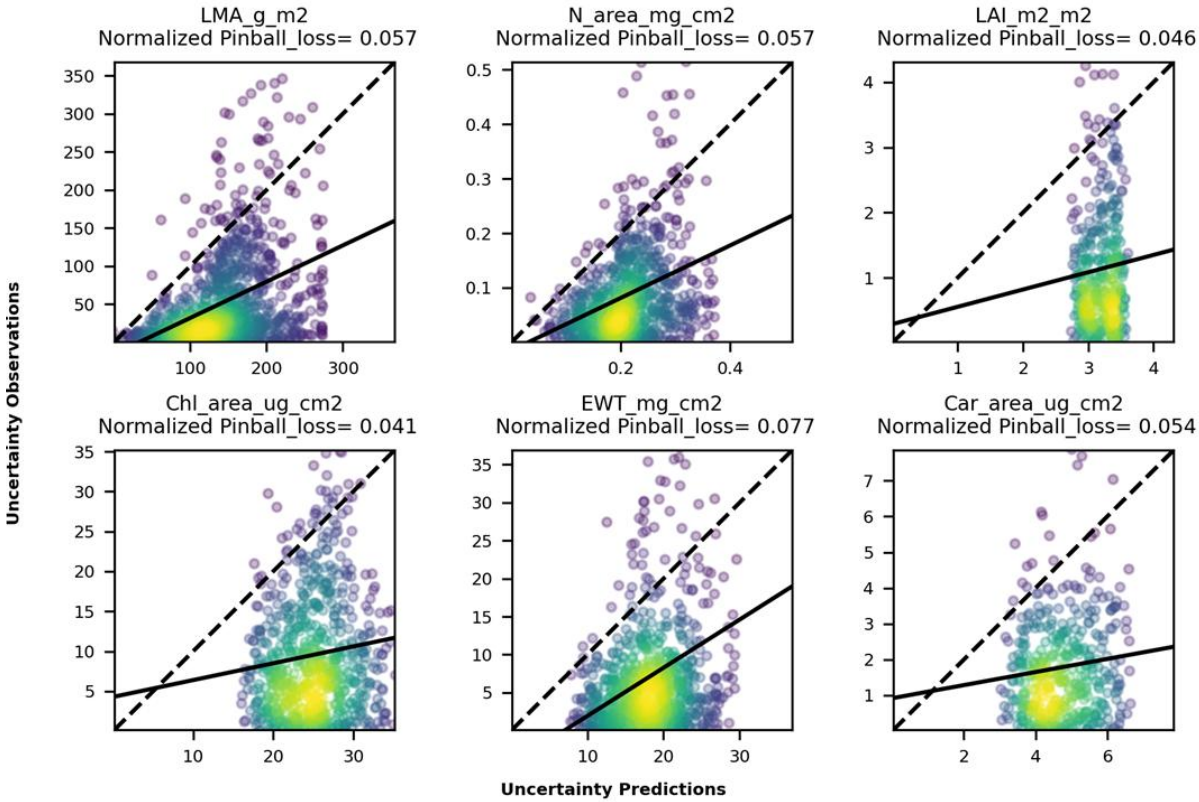

Figure S4: Correlation between observed and predicted values of six traits: Leaf Mass per Area (LMA), Nitrogen content (N), Leaf Area Index (LAI), Chlorophyll content (Chl), Equivalent Water Thickness (EWT), and Carotenoid content (Car) from the Dis_UN model

Table S5: The Expected Normalized Calibration Error (ENCE) values for the three compared uncertainty methods: the distance based method (Dis_UN), ensemble deep learning (Ens_UN) and monte carlo drop-out method (MCDrop_UN)

Traits	Dist_UN	Ens_Un	Mcdrop_UN
LMA	0.519	1.669	17.591
N	0.441	1.821	14.995
LAI	0.531	1.19	9.761
Chl	0.503	1.361	8.55
EWT	0.533	2.237	12.494
Car	0.5	1.401	7.778

Table S6: The regression coefficients of each scaled predictor for all the six traits: Leaf Mass per Area (LMA), Nitrogen content (N), Leaf Area Index (LAI), Chlorophyll content (Chl), Equivalent Water Thickness (EWT), and Carotenoid content (Car)

	LMA	**N**	**LAI**	**Chl**	**EWT**	**Car**
Intercept	139.1837	0.211816	3.204911	24.83733	17.99426	4.691486
Distance embedding space	7.071657	0.001075	-0.13865	1.821151	0.86472	0.104252
Distance feature space	53.74244	0.063145	-0.12674	3.461149	4.355728	0.812609

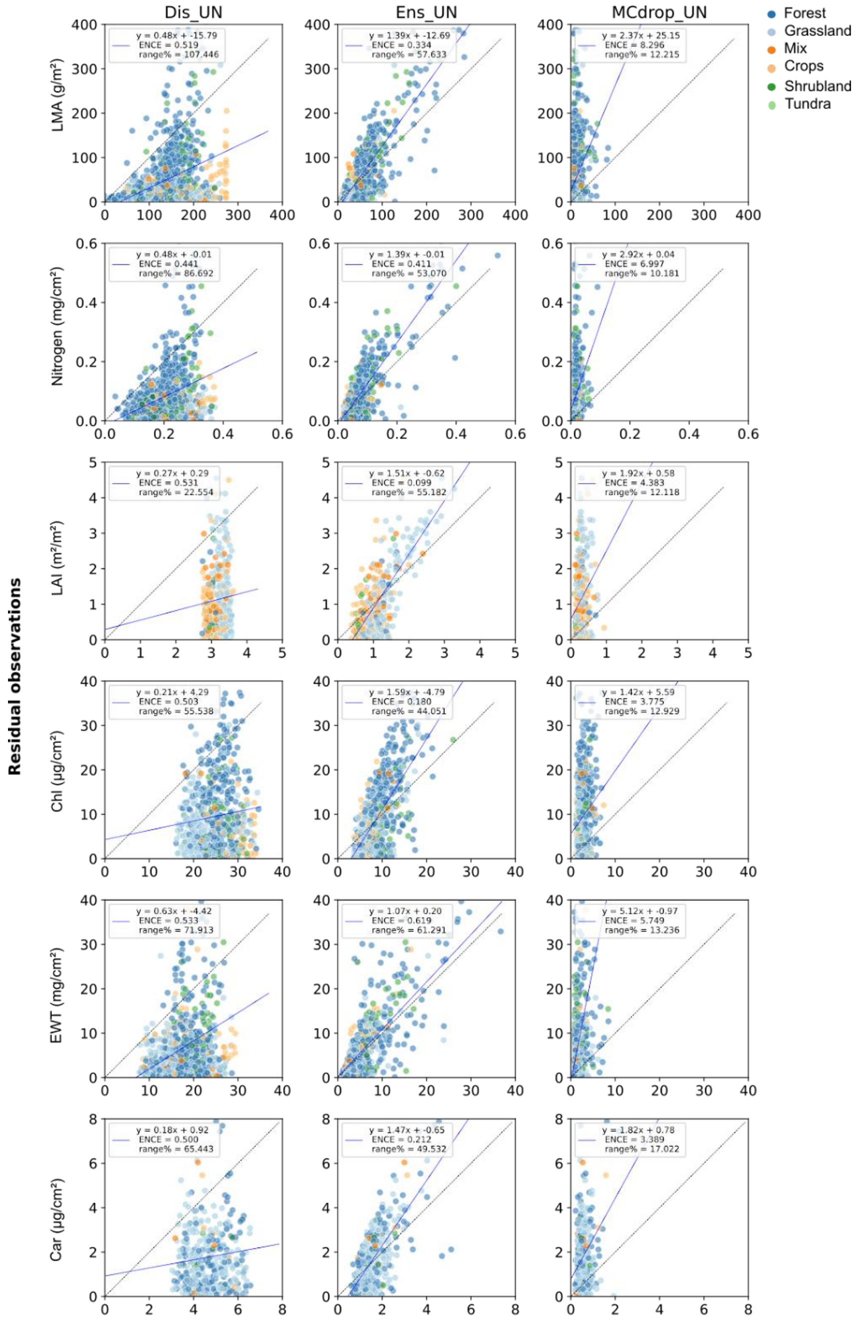

Figure S5: Scatter plots comparing the predicted uncertainties from three methods—distance-based (Dis_UN), ensemble (Ens_UN), and Monte Carlo dropout (MCdrop_UN) , defined as 2 × standard deviation to cover 95% confidence intervals) —against observed residuals of the multi-trait models across six traits: Leaf Mass per Area (LMA), Nitrogen content, Chlorophyll content (Chl), Equivalent Water Thickness (EWT), Leaf Area Index (LAI), and Carotenoid content (Car). For evaluation we show the Expected Normalized Calibration Error metric (ENCE) and well as the ratio of predicted and observed ranges.

Supplement of uncertainty predictions and evaluation

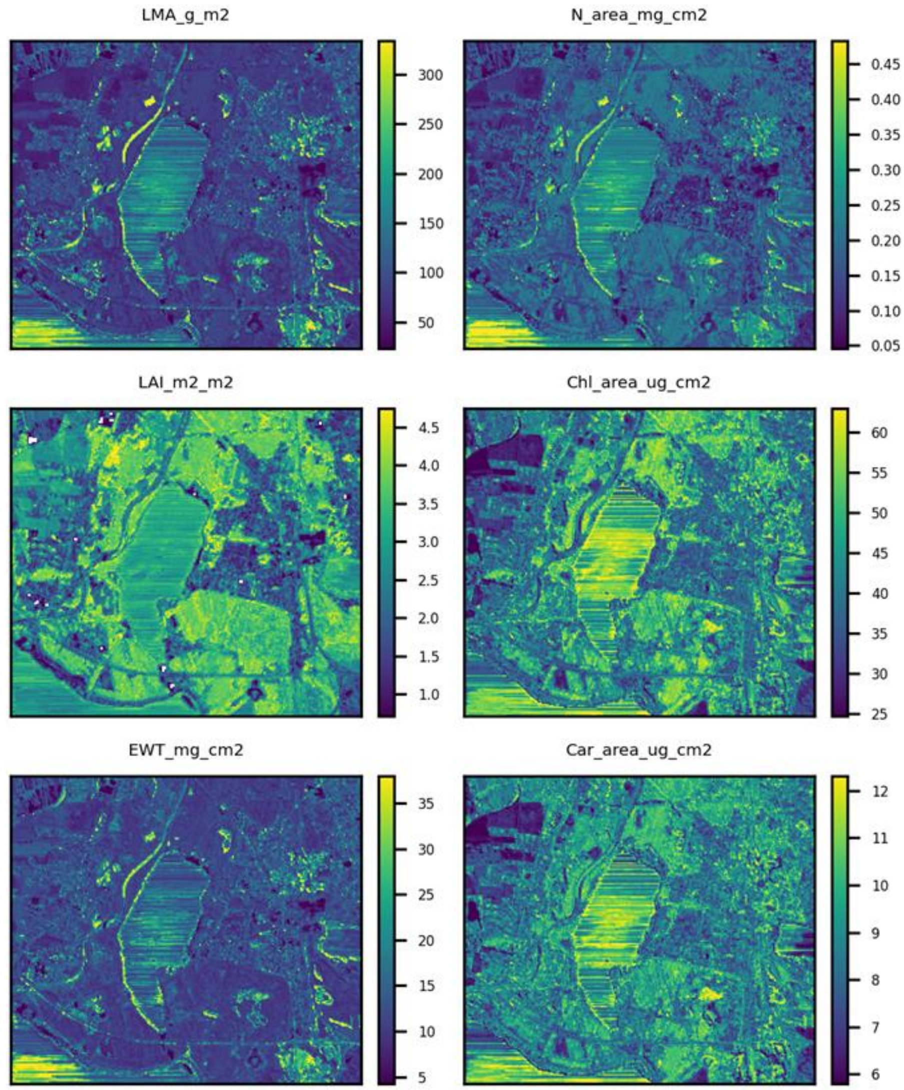

Figure S6: The predicted trait values from the multi-trait for six traits (Leaf Mass per Area (LMA), Nitrogen content, Chlorophyll content (Chl), Equivalent Water Thickness (EWT), Leaf Area Index (LAI), and Carotenoid content (Car)) when applied on the EnMAP scene.

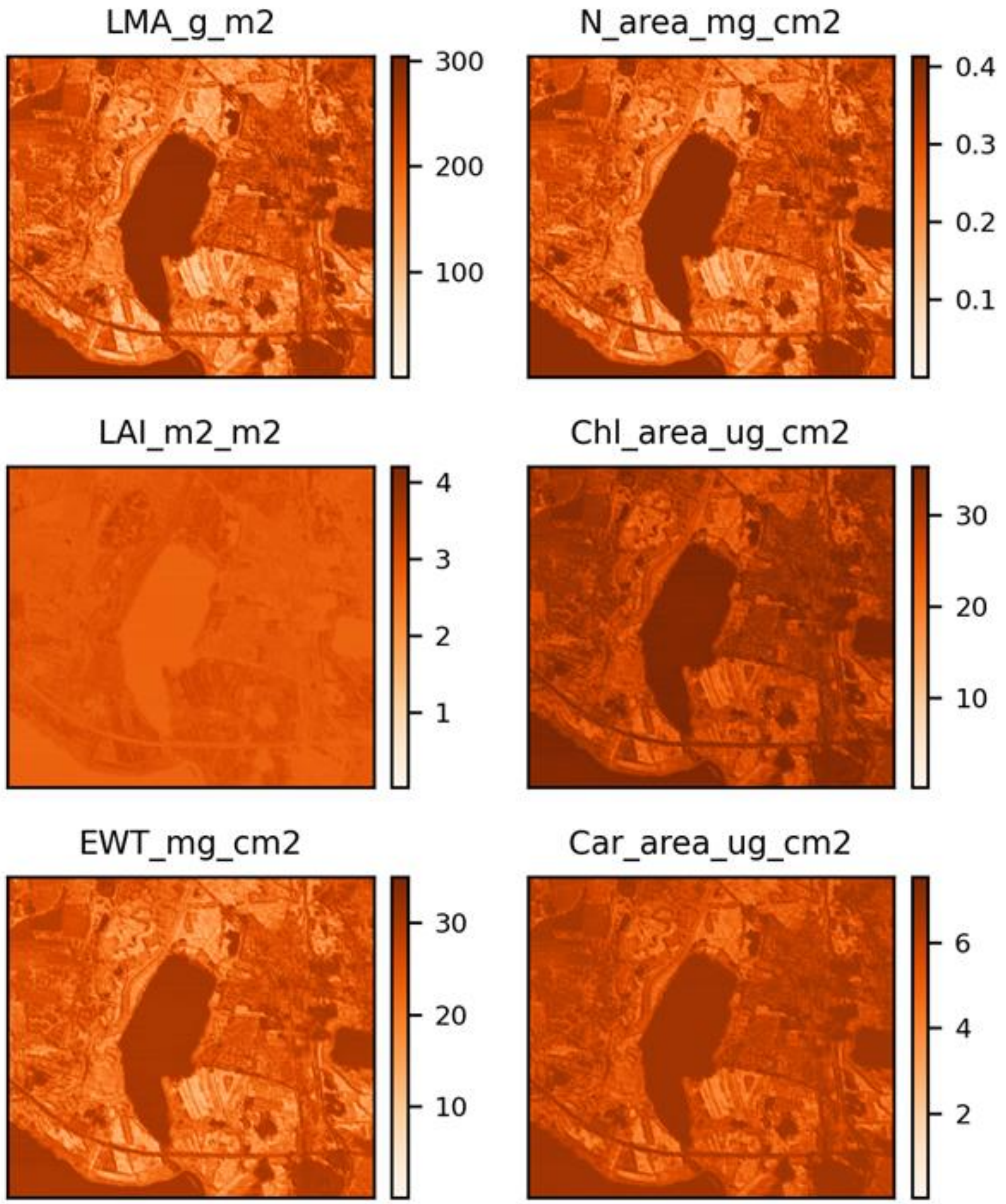

145 **Figure S7: The predicted uncertainty values from the Dis_UN method for six traits (Leaf Mass per Area (LMA), Nitrogen content, Chlorophyll content (Chl), Equivalent Water Thickness (EWT), Leaf Area Index (LAI), and Carotenoid content (Car)) when applied on the EnMAP scene. The is a supplement to Fig. 4 where the color bar ranges use the range of training data as basis.**

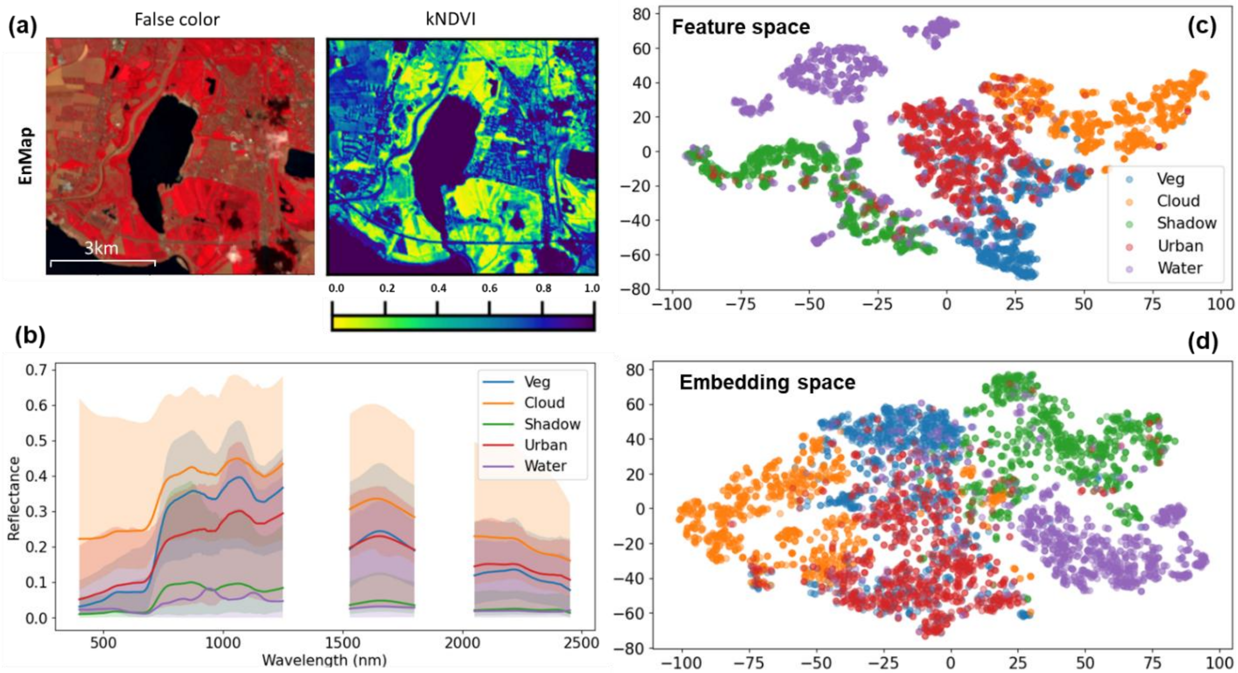

Figure S8a: Visualization of 1000 sampled pixels from each scene component from the EnMAP scene: (a) Characteristics of the scene (b) Distribution of canopy reflectance (c) T-SNE visualization of the spectra in the feature space (d) T-SNE visualization of the spectra in the embedding space of the multi-trait model.

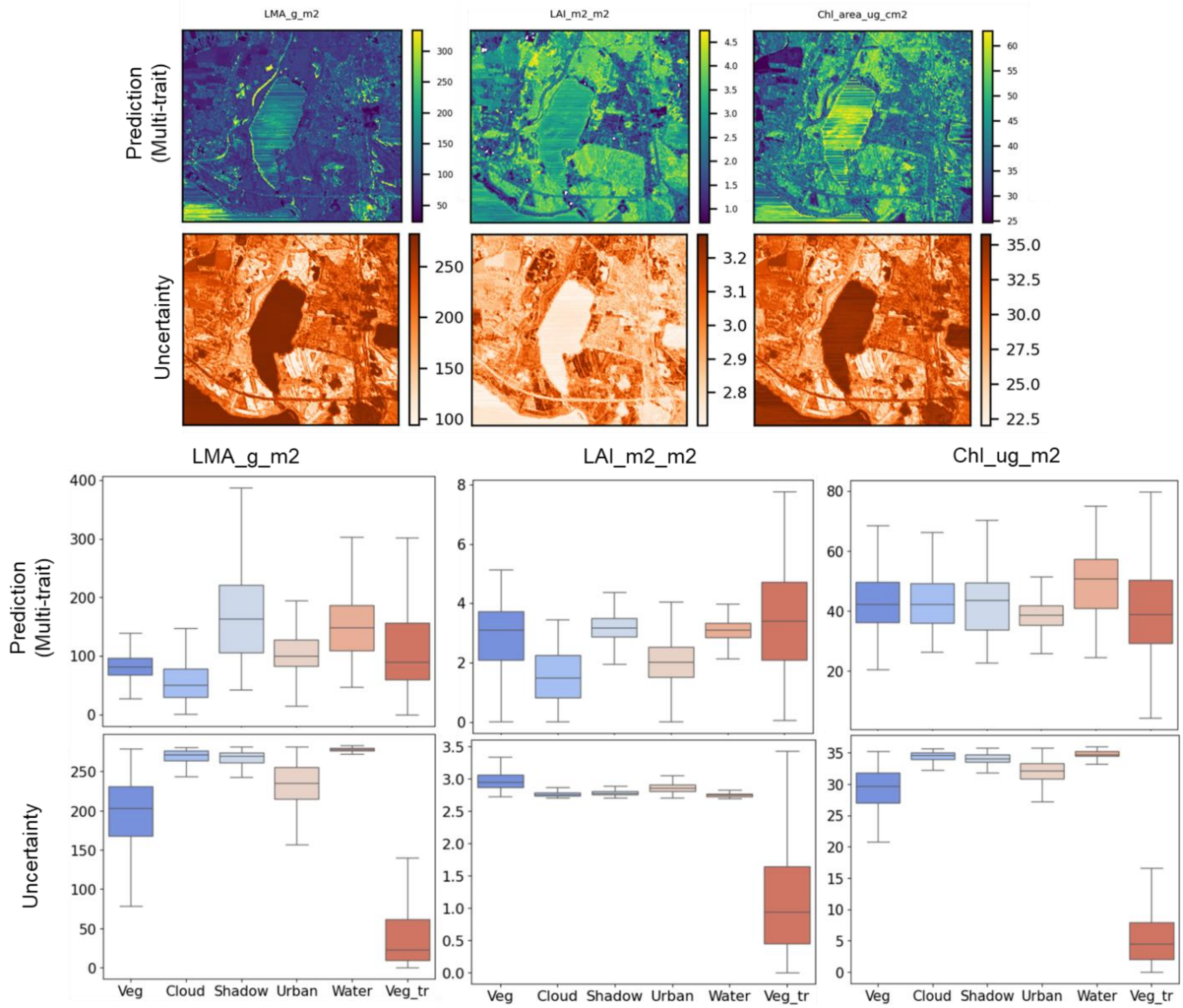

Figure S8b: Comparison of distribution in the trait predicted values from the multi-trait model and the predicted uncertainty values from the Dis_UN when applied on sampled pixels shown in Fig. 8a

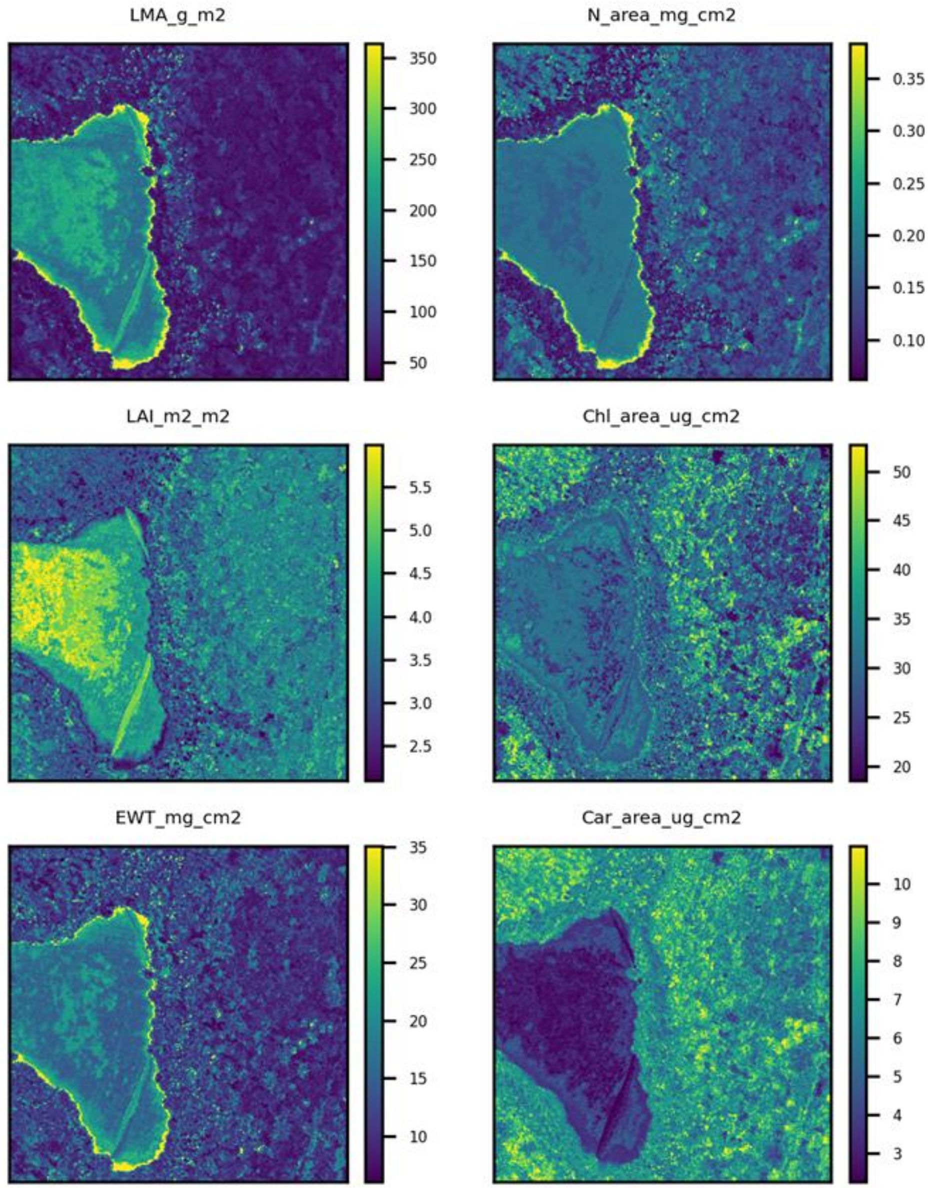

Figure S9: The predicted trait values from the multi-trait for six traits (Leaf Mass per Area (LMA), Nitrogen content, Chlorophyll content (Chl), Equivalent Water Thickness (EWT), Leaf Area Index (LAI), and Carotenoid content (Car)) when applied on the NEON scene.

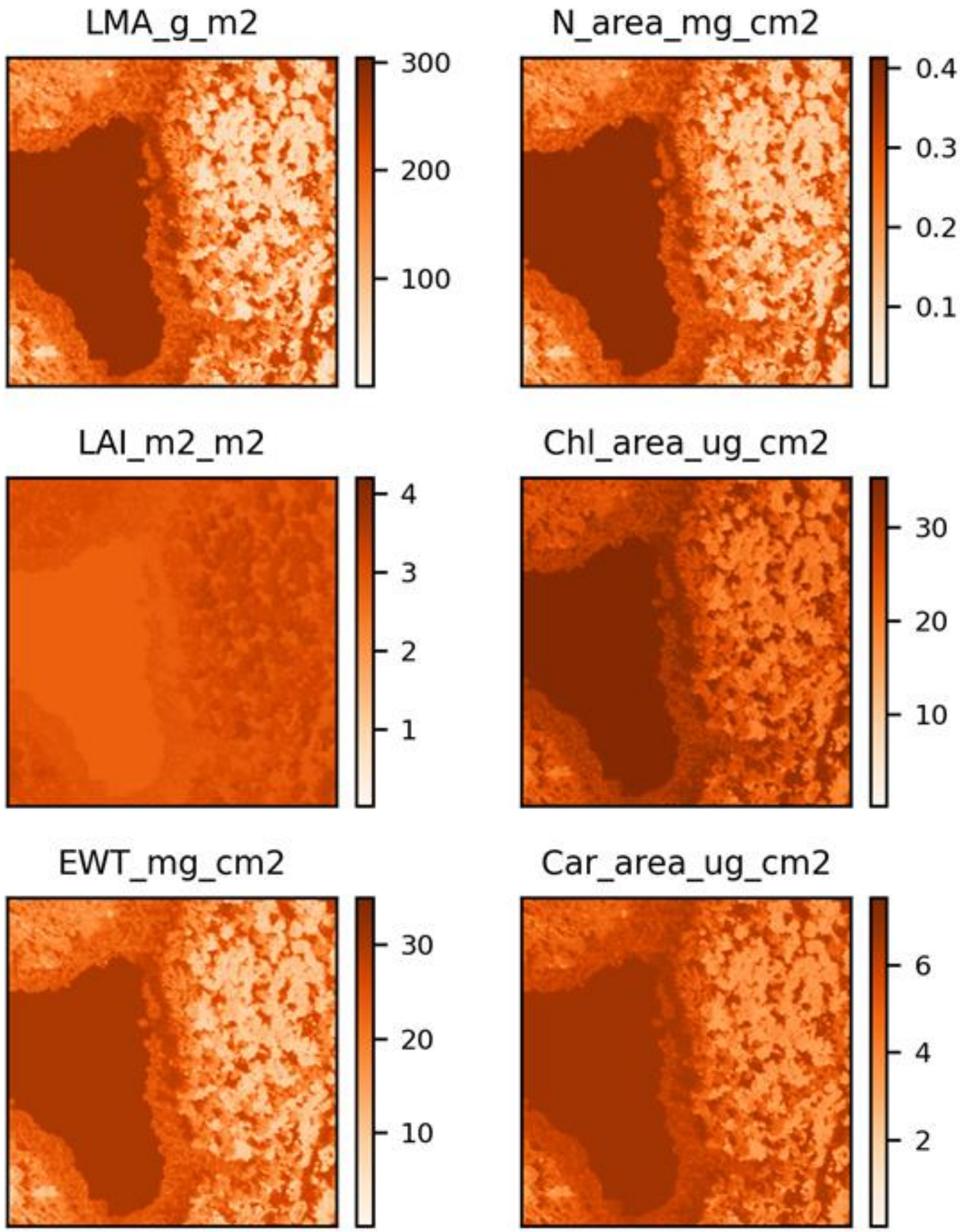

Figure S10: The predicted uncertainty values from the Dis_UN method for six traits (Leaf Mass per Area (LMA), Nitrogen content, Chlorophyll content (Chl), Equivalent Water Thickness (EWT), Leaf Area Index (LAI), and Carotenoid content (Car)) when applied on the NEON scene. The is a supplement to Fig. 5 where the color bar ranges use the range of training data as basis.

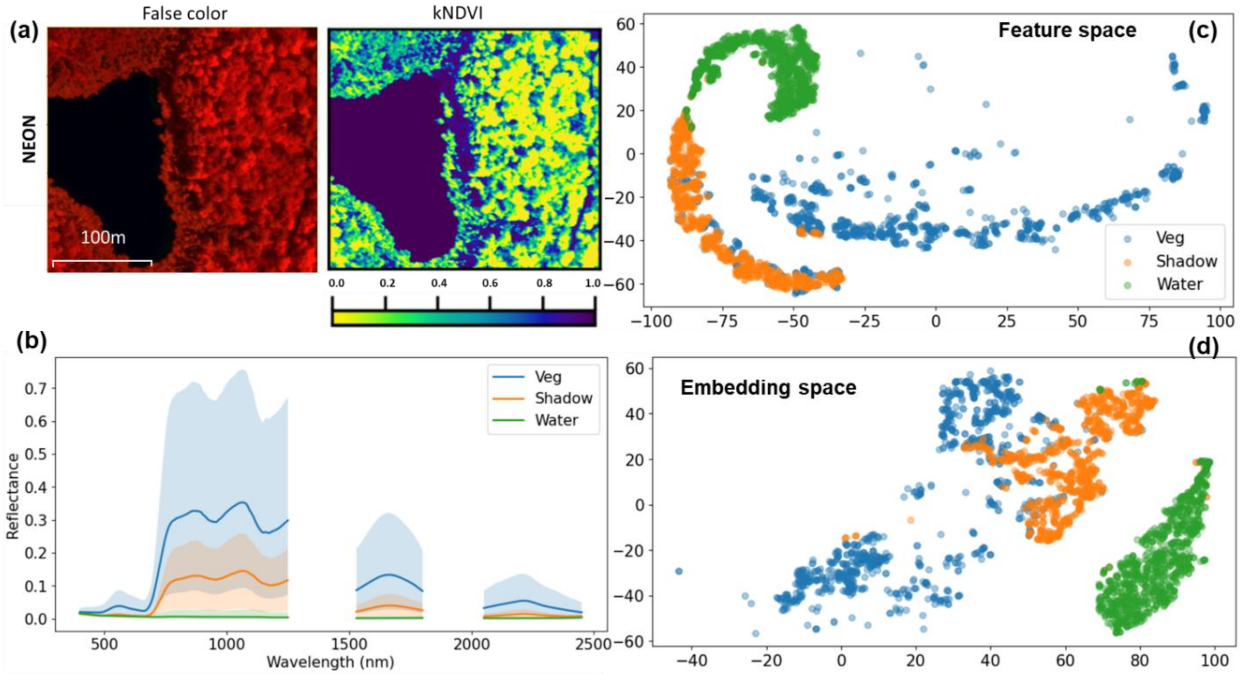

Figure S11a: Visualization of 1000 sampled pixels from each scene component from the NEON scene: (a) Characteristics of the scene (b) Distribution of canopy reflectance (c) T-SNE visualization of the spectra in the feature space (d) T-SNE visualization of the spectra in the embedding space of the Multi-trait model.

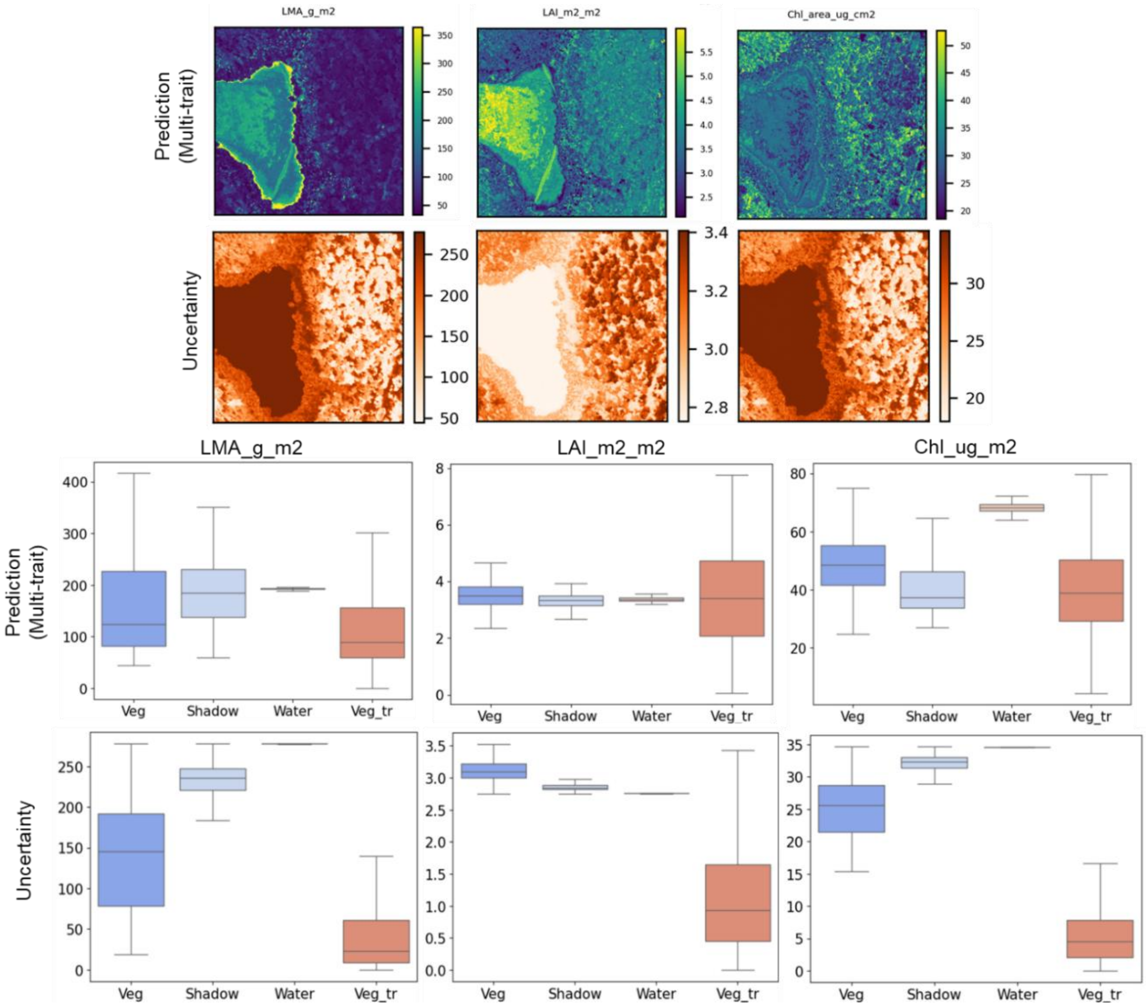

Figure S11b: Comparison of distribution in the trait predicted values from the multi-trait model and the predicted uncertainty values from the Dis_UN when applied on sampled pixels shown in Fig. C6a

Supplement of the comparison with state-of-the-art methods

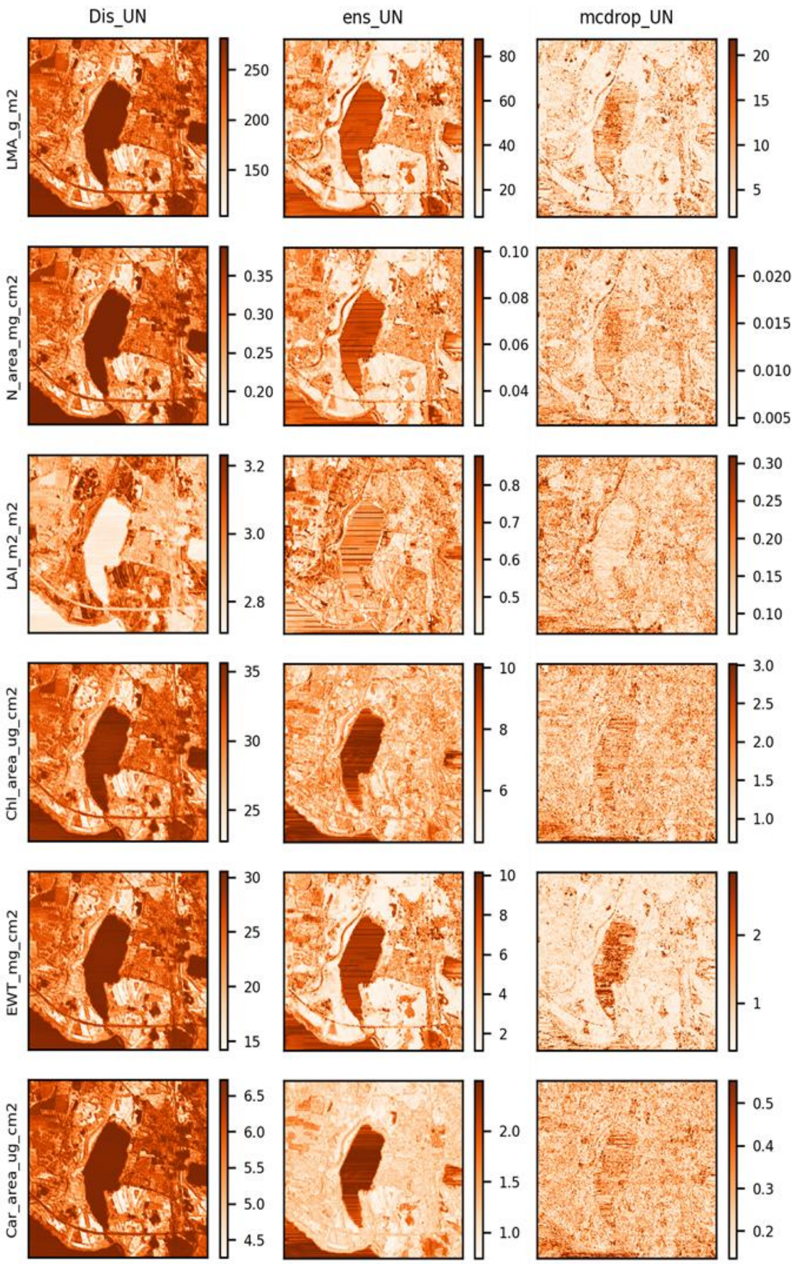

Figure S12a: EnMAP scene: Comparison of uncertainty estimations for six traits Leaf Mass per Area (LMA), Nitrogen content, Chlorophyll content (Chl), Equivalent Water Thickness (EWT), Leaf Area Index (LAI), and Carotenoid content (Car) using three methods: Distance-based (Dis_UN), Ensemble (ens_UN), and Monte Carlo dropout (mcdrop_UN). Spatial maps show the uncertainty distribution for each method.

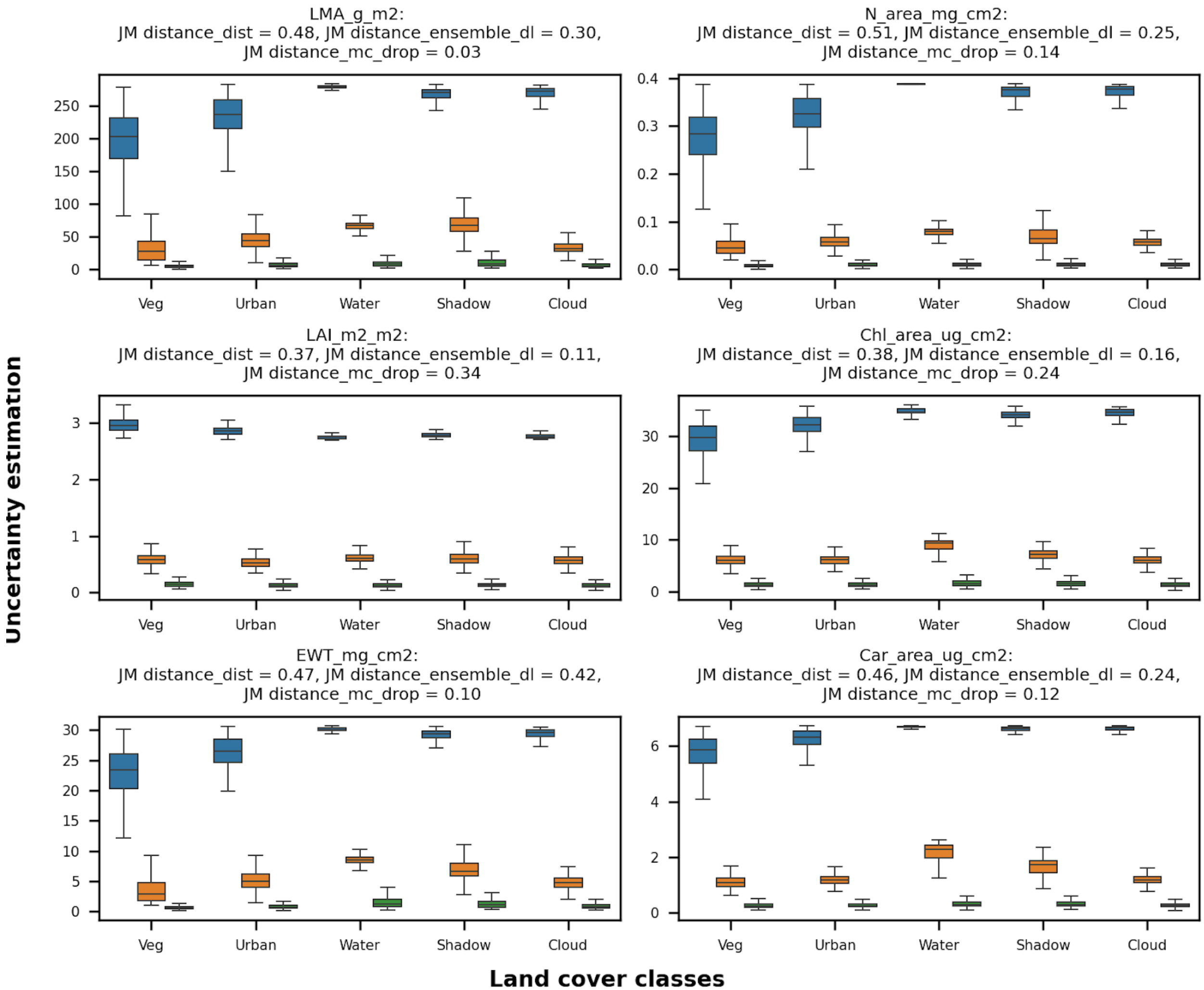

Figure S12b: EnMAP scene: Comparison of uncertainty estimations for six traits Leaf mass per area Leaf Mass per Area (LMA), Nitrogen content, Chlorophyll content (Chl), Equivalent Water Thickness (EWT), Leaf Area Index (LAI), and Carotenoid content (Car) using three methods: Distance-based (Dis_UN), Ensemble (ens_UN), and Monte Carlo dropout (mcdrop_UN). Box plots show uncertainty distributions across different scene components (Vegetation, Urban, Water, Shadow and Cloud) for each method. Jeffries Matusita (JM) distances and Kolmogorov-Smirnov (KS) tests quantify the separability of vegetated pixels with non-vegetated classes.

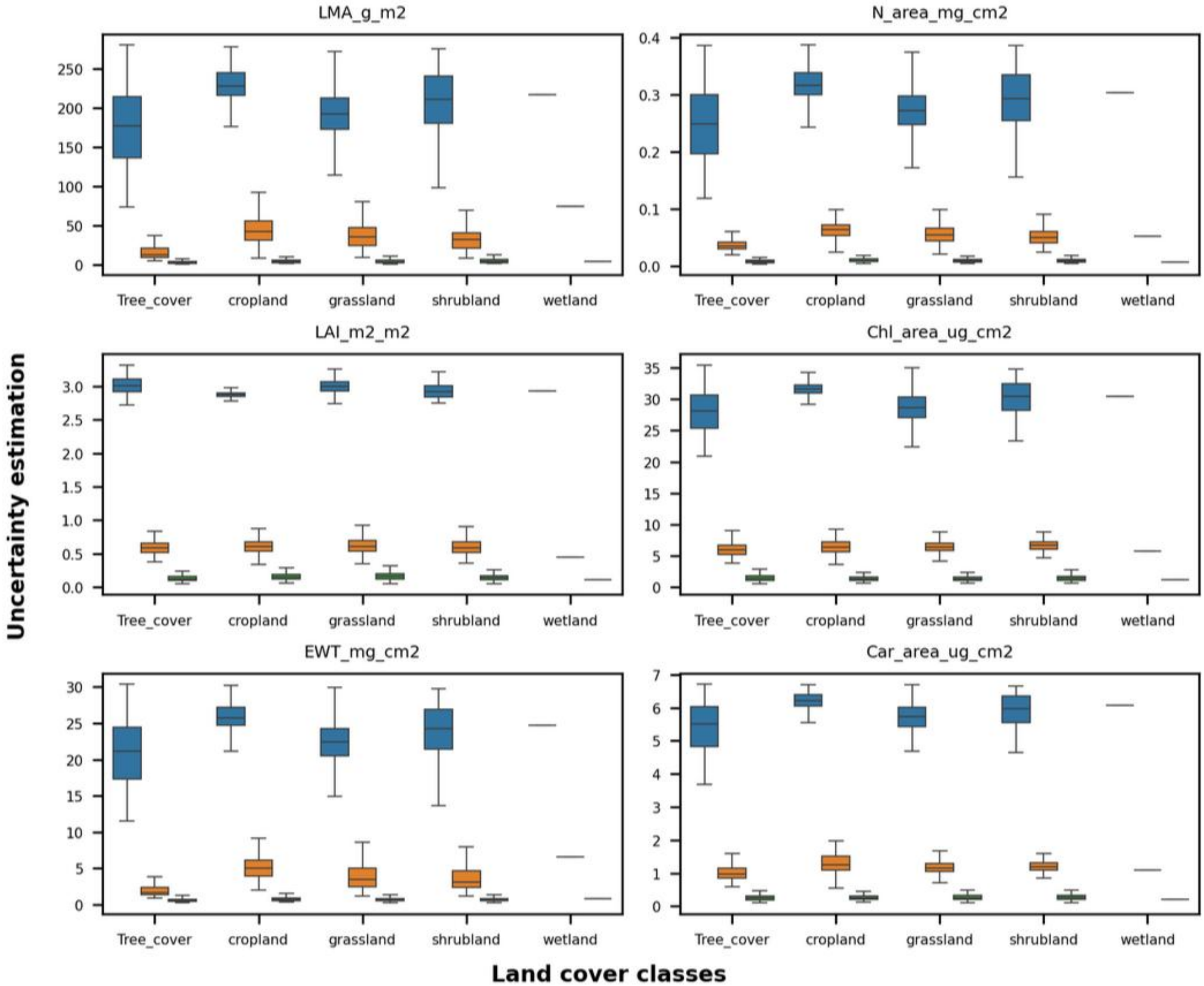

Figure S13: EnMAP scene: Comparison of uncertainty estimations for six traits Leaf mass per area (LMA), Chlorophyll (Chl), Carotenoids (Car), Nitrogen (N) content, Leaf area index (LAI) and Equivalent water thickness (EWT) using three methods: Distance-based (Dis_UN), Ensemble (ens_UN), and Monte Carlo dropout (mcdrop_UN). Box plots show uncertainty distributions across different Vegetation types for each method.

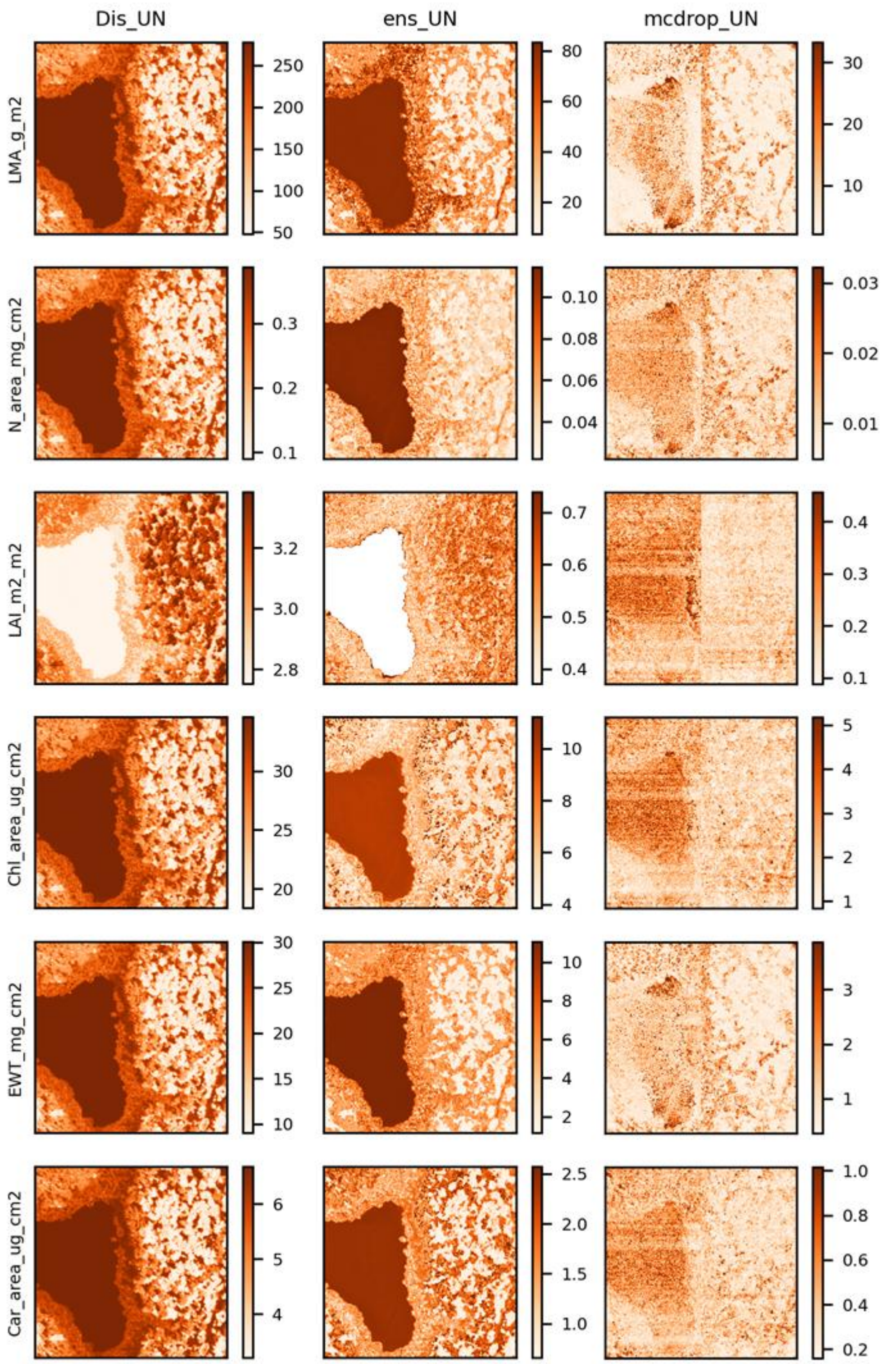

Figure S14a: Neon scene: Comparison of uncertainty estimations for six traits Leaf mass per area (LMA), Chlorophyll (Chl), Carotenoids (Car), Nitrogen (N) content, Leaf area index (LAI) and Equivalent water thickness (EWT) using three methods: Distance-based (Dis_UN), Ensemble (ens_UN), and Monte Carlo dropout (mcdrop_UN). Spatial maps show the uncertainty distribution for each method.

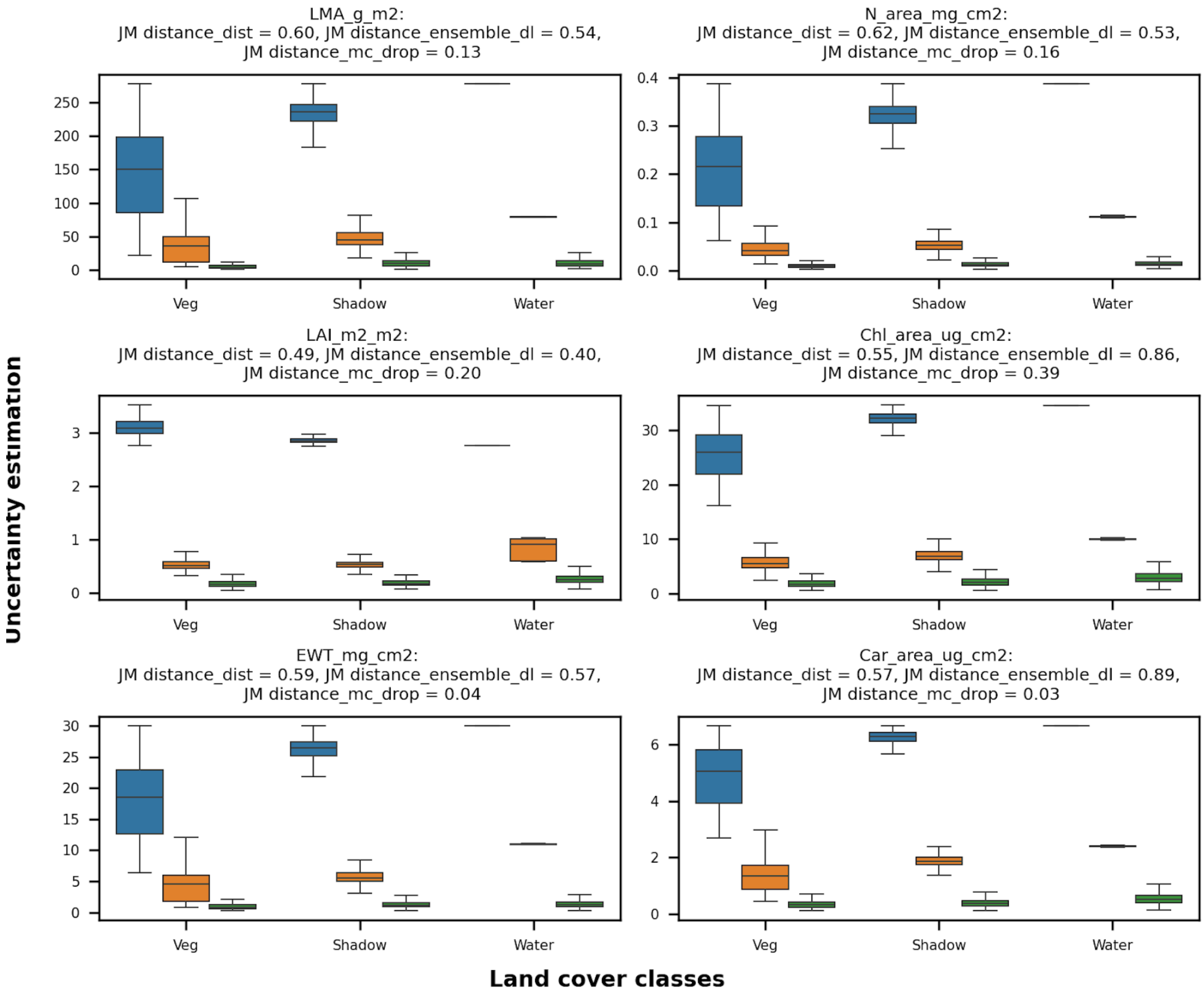

Figure S14b: Neon scene: Comparison of uncertainty estimations for six traits Leaf mass per area (LMA), Chlorophyll (Chl), Carotenoids (Car), Nitrogen (N) content, Leaf area index (LAI) and Equivalent water thickness (EWT) using three methods: Distance-based (Dis_UN), Ensemble (ens_UN), and Monte Carlo dropout (mcdrop_UN). Box plots show uncertainty distributions across different scene components (Vegetation, Shadow, Water) for each method. Jeffries Matusita (JM) distances and Kolmogorov-Smirnov (KS) tests quantify the separability of vegetated pixels with non-vegetated classes.